The Plant Journal (2006) **45**, 31–45 doi: 10.1111/j.1365-313X.2005.02590.x

Tomato *Pto* encodes a functional *N*-myristoylation motif that is required for signal transduction in *Nicotiana benthamiana*

Jeroen S. de Vries, Vasilios M.E. Andriotis, Ai-Jiuan Wu and John P. Rathjen*
The Sainsbury Laboratory, John Innes Centre, Colney Lane, Norwich, NR4 7UH, UK

Received 5 May 2005; revised 5 September 2005; accepted 7 September 2005.
*For correspondence (fax +44 1603 450011; e-mail john.rathjen@sainsbury-laboratory.ac.uk).

Summary

Pto kinase of tomato (*Lycopersicon esculentum*) confers resistance to bacterial speck disease caused by *Pseudomonas syringae* pv. *tomato* expressing *avrPto* or *avrPtoB*. Pto interacts directly with these type-III secreted effectors, leading to induction of defence responses including the hypersensitive response (HR). Signalling by Pto requires the nucleotide-binding site–leucine-rich repeat (NBS–LRR) protein Prf. Little is known of how Pto is controlled prior to or during stimulation, although kinase activity is required for Avr-dependent activation. Here we demonstrate a role for the *N*-terminus in signalling by Pto. *N*-terminal residues outside the kinase domain were required for induction of the HR in *Nicotiana benthamiana*. The *N*-terminus also contributed to both AvrPto-binding and phosphorylation abilities. Pto residues 1–10 comprise a consensus motif for covalent attachment of myristate, a hydrophobic 14-carbon saturated fatty acid, to the Gly-2 residue. Several lines of evidence indicate that this motif is important for Pto function. A heterologous *N*-myristoylation motif complemented *N*-terminal deletion mutants of Pto for *Prf*-dependent signalling. Signalling by wild-type and mutant forms of Pto was strictly dependent on the Gly-2 residue. The *N*-myristoylation motif of Pto complemented the cognate motif of AvrPto for avirulence function and membrane association. Furthermore, Pto was myristoylated *in vivo* dependent on the presence of Gly-2. The subcellular localization of Pto was independent of *N*-myristoylation, indicating that *N*-myristoylation is required for some function other than membrane affinity. Consistent with this idea, AvrPtoB was also found to be a soluble protein. The data indicate an important role(s) for the myristoylated *N*-terminus in Pto signalling.

Keywords: Pto kinase, disease resistance, tomato, *N*-mytistoylation, signal transduction, *N. benthamiana*.

Introduction

Plants detect potential disease-causing organisms through recognition events specified by cognate resistance (*R*) and avirulence (*Avr*) genes in host and pathogen, respectively (Flor, 1971). The molecular mechanisms underlying such 'gene-for-gene' phenomena are not well understood, but Avr products are believed to elicit signal transduction pathways in which R proteins are the most important regulatory molecules (Baker *et al.*, 1997). Several classes of R protein have been identified, and most possess leucine-rich repeat (LRR) motifs. For extracellular R proteins, the LRRs are perfect and precede a transmembrane domain (Jones and Jones, 1996). For intracellular R proteins, the LRRs are imperfect and always paired with an amino-terminal nucleotide-binding site (NBS–LRR) domain. Conversely, Avr proteins are characteristically diverse with the exception that proteases are highly represented in this class (Rathjen and Moffett, 2003).

Elicitation of signal transduction leads to induction of local defences, often accompanied by a cell-death phenotype known as the hypersensitive response (HR), and a systemic response (Hammond-Kosack and Jones, 1996). Most current explanations of the gene-for-gene interaction treat the Avr as an elicitor that activates a host receptor or receptor complex (Belkhadir *et al.*, 2004a,b; Dangl and Jones, 2001). Differences between the models centre on whether the R protein comprises the receptor itself, or is a component of a receptor–protein complex which detects the Avr indirectly, for example via a proximal Avr receptor or by secondary detection of an Avr-modified host protein (Axtell and Staskawicz, 2003; Mackey *et al.*, 2002, 2003). Examples

© 2005 The Authors
Journal compilation © 2005 Blackwell Publishing Ltd

of direct contact between R and Avr components include the interaction between the NBS–LRR protein Pi-ta and the cognate Avr-Pita protease, and between the NBS–LRR protein RRS-1R and its cognate PopP2 protease (Deslandes *et al.*, 2003; Jia *et al.*, 2000). Conversely, several R proteins of *Arabidopsis thaliana* appear to fit an indirect model of interaction. Degradation of the *A. thaliana* protein RIN4 by AvrRpt2 is sufficient for activation of RPS2 (Axtell and Staskawicz, 2003; Mackey *et al.*, 2003). RIN4 also interacts with AvrB and AvrRpm1, and is required for accumulation of the cognate RPM1 protein, but the mechanism of RPM1 activation apparently differs from RPS2 (Belkhadir *et al.*, 2004a,b; Mackey *et al.*, 2002, 2003). The protease AvrPphB activates signalling by RPS5 on cleavage of the PBS1 kinase domain, but how this event contributes to signalling is unclear (Shao *et al.*, 2003).

The avirulence proteins AvrPto and AvrPtoB of *Pseudomonas syringae* pv. *tomato* (*Pst*) activate disease resistance in tomato cultivars harbouring the *Pto* gene (Kim *et al.*, 2002; Martin *et al.*, 1993; Ronald *et al.*, 1992). These Avr proteins are secreted by the type III secretion system of *Pst*, and are believed to interact with Pto directly upon deposition in the plant cell (Kim *et al.*, 2002; Pedley and Martin, 2003; Scofield *et al.*, 1996; Tang *et al.*, 1996). AvrPto and AvrPtoB are unrelated at the amino acid level; despite this, they interact with the same patch of residues on the surface of the Pto kinase domain (Kim *et al.*, 2002; Wu *et al.*, 2004). AvrPto consists of 164 amino acids, a core of which folds into an extended anti-parallel three-helix bundle (Wulf *et al.*, 2004). AvrPto is bound to the plasma membrane upon modification with myristate in the host cell (Shan *et al.*, 2000). Conversely, AvrPtoB does not possess an *N*-myristoylation motif, and has not been reported to be associated with a cell membrane (Kim *et al.*, 2002). Activation of Pto by AvrPto or AvrPtoB stimulates a signal transduction pathway that requires the NBS–LRR protein Prf, culminating in induction of defence responses including the HR (Pedley and Martin, 2003).

Protein *N*-myristoylation involves the covalent attachment of a hydrophobic 14-carbon saturated fatty acid to the glycine at residue two (Gly-2) (Boutin, 1997; Farazi *et al.*, 2001; Johnson *et al.*, 1994). *N*-myristoylation of *A. thaliana* protein substrates requires the consensus sequence: M-G-X {not EDFKRVWY}-X-X- [STACFGRV]-X {not DE}, where X is any amino acid (Boisson *et al.*, 2003). *N*-myristoylation of proteins can fulfil several functions. The most common role is to confer membrane association by enhancement of hydrophobic membrane–protein interactions (Resh, 1999). For example, *N*-myristoylation provides the primary membrane-targeting signal for several plant protein kinases (Martin and Busconi, 2000; Murase *et al.*, 2004). Evidence is also accumulating that the myristate moiety itself may participate in intra- or intermolecular interactions with proteins. The non-receptor tyrosine kinase c-Abl is autoinhibited by its myristoylated *N*-terminus, which is sequestered in a hydrophobic pocket in the *C*-terminal lobe of the kinase domain (Hantschel *et al.*, 2003). Intermolecular myristate–protein interactions contribute to assemblage of structural proteins of the poliovirus virion (Chow *et al.*, 1987; Moscufo and Chow, 1992). Similarly, myristoylation enhances the interaction between calmodulin and several proteins (Hayashi *et al.*, 2002; Matsubara *et al.*, 2003; Ulrich *et al.*, 2000).

Pto is a member of a small gene family in *Lycopersicon* spp. which includes *Fen*, *Pth2*, *Pth3*, *Pth4* and *Pth5* (Chang *et al.*, 2002; Riely and Martin, 2001; Vleeshouwers *et al.*, 2001). These genes reside together with *Prf* at a locus on chromosome 5 (Chang *et al.*, 2002; Salmeron *et al.*, 1996). *Pto*, *Pth3*, *Pth5* and *Fen* are all able to elicit HR-like cell death dependent on the presence of the *Prf* gene. All *Pto* homologues, with the exception of *Pth4*, encode consensus myristoylation motifs in their respective *N*-termini (Chang *et al.*, 2002; Martin *et al.*, 1993; Riely and Martin, 2001; Rommens *et al.*, 1995). Fen required the myristoylation site Gly-2 for fenthion sensitivity in transient gene-expression assays in tomato (Rommens *et al.*, 1995). A peptide corresponding to the identical nine amino-terminal residues of Fen and Pto was an efficient substrate for *N*-myristoyl transferase from *A. thaliana* (Qi *et al.*, 2000). In contrast, Pto-mediated disease resistance was not compromised by mutation of the Gly-2 residue to Ala (Loh *et al.*, 1998). Thus the data concerning a role for *N*-myristoylation in signalling by Pto family members are inconsistent.

We recently identified a patch of residues on the surface of Pto required for interaction with both AvrPto and AvrPtoB in yeast (Wu *et al.*, 2004). This patch appears to be an important point of regulatory convergence for Pto, because it overlaps the catalytic cleft of the kinase. Moreover, we identified a negative regulatory patch within the Avr-interaction region. Mutations within this area conferred a constitutive gain-of-function (CGF) phenotype of Avr-independent cell death when the proteins were expressed in *Nicotiana benthamiana*. We synthesized a model in which the catalytic cleft of Pto is occupied by a negative regulatory molecule which suppresses signalling. Avr binding causes displacement of the inhibitory peptide from the kinase catalytic cleft, allowing a regulatory phosphorylation event leading to its permanent removal. Release of the negative regulator is sufficient for activation, because kinase activity is dispensable after this step. The identity of the putative regulator is unknown, but could be part of Pto itself, or an unknown molecule.

Here we examine a role for the amino-terminal non-kinase residues of Pto in signal transduction. We reasoned that identification of the negative regulatory patch does not completely account for regulation, because Pto also contributes positively to signalling. In addition to the well characterized kinase domain, *Pto* encodes approximately 40 amino-terminal residues with no defined function. Here we

© 2005 The Authors
Journal compilation © 2005 Blackwell Publishing Ltd,

show that residues 1–30 are required for signalling, which was partially explained by altered abilities of the deletion mutants to interact with Avr proteins or catalyse phosphotransfer. However, residues 1–10, which constitute the consensus *N*-myristoylation motif, were dispensable for ligand binding and kinase activity. We show that the Pto *N*-myristoylation motif complemented the cognate motif of AvrPto for avirulence activity and plasma membrane localization, and that Pto is a myristoylated protein *in vivo*. Despite these observations, Pto was a soluble cytoplasmic protein irrespective of *N*-myristoylation status. Similarly to Pto, AvrPtoB appeared to be a soluble protein. The data are consistent with a requirement for *N*-myristoylation of Pto during signal transduction in *N. benthamiana*.

Results

Pto amino acids 1–10 are required for induction of the AvrPto-dependent HR and CGF phenotype in N. benthamiana

To examine a role for the Pto *N*-terminus in signalling, we created a set of *N*-terminal deletions of wild-type Pto and the CGF mutant pto^{L205D} (Wu *et al.*, 2004). Wild-type and mutant *Pto* genes were truncated to remove coding capacity for 10, 20 or 30 amino acids, cloned into binary vectors under control of the strong constitutive CaMV 35S promoter, and fused genetically to a *C*-terminal FLAG epitope. We used *Agrobacterium tumefaciens* to express each gene transiently in *N. benthamiana* leaves. *Nicotiana benthamiana* supports *avrPto*-dependent signalling by tomato *Pto* in a *Prf*-dependent manner, and the transgenic line 291-2 expresses *avrPto* upon induction by dexamethasone (DEX; Chang *et al.*, 2002; Lu *et al.*, 2003). Transient expression of *Pto*, *pto[N-10]*, *pto[N-20]*, or *pto[N-30]* in *N. benthamiana* 291–2 leaves did not lead to cell death in the absence of DEX (data not shown). Application of DEX to the areas infiltrated with *Agrobacterium* resulted in HR in the wild-type control within 2 days post-infiltration (Figure 1a). In contrast to wild-type Pto, DEX treatment of tissue transformed with any deletion mutant or the empty vector did not lead to the HR (Figure 1a). Therefore *N*-terminal residues 1–10 of Pto are required for signalling of the AvrPto-dependent HR. The lack of HR by deletion mutants was not due to instability of the expressed protein, because Western blotting of total protein extracts from infiltrated leaves with specific antisera

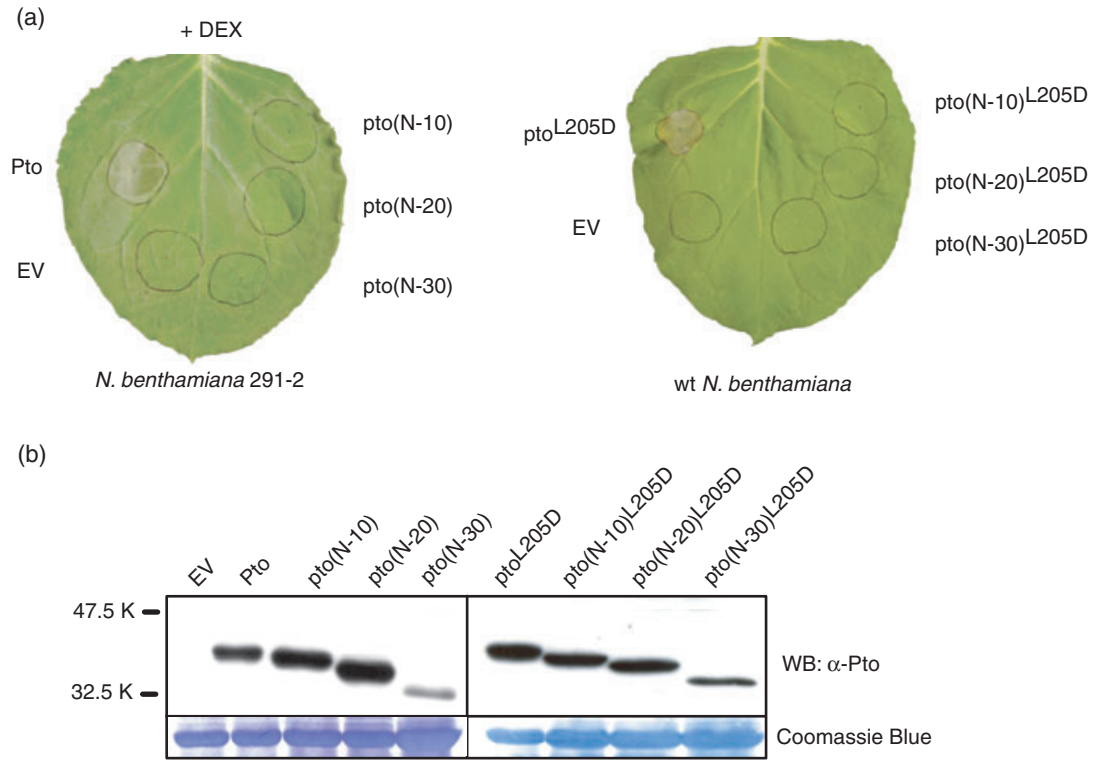

Figure 1. Pto amino acids N1–10 are required for the AvrPto-dependent and CGF HR phenotypes in *Nicotiana benthamiana*.
(a) Transient expression of *N*-terminal deletion mutants of Pto in *N. benthamiana* line 291-2 or in wild-type (wt) *N. benthamiana*. Leaves were infiltrated with *Agrobacterium* containing each construct as indicated. The area of infiltration was outlined with a marker pen. Line 291-2 was treated with DEX to induce avrPto expression. Leaves are shown 4 days after infiltration. EV, empty vector control.
(b) Accumulation of mutant pto proteins *in planta*. Total protein was extracted from leaves and blotted against polyclonal anti-Pto antisera after SDS-PAGE. Bottom panel, equivalent loading by Coomassie Blue staining of the Western blot membrane.

© 2005 The Authors

confirmed the accumulation of all mutant proteins (Figure 1b). The pto[N-30] mutant accumulated to a lower level compared with the other *N*-terminal deletion mutants. Similarly to deletion mutants of wild-type Pto, transient expression of *pto*[N-10]^{L205D}, *pto*[N-*20*]^{L205D}, or *pto*[N-*30*]^{L205D} in wild-type *N. benthamiana* leaves did not induce cell death, whereas expression of the original CGF mutant *pto*^{L205D} led to confluent HR within the infiltrated area within 48 h (Figure 1a). Protein accumulated upon expression of all mutants (Figure 1b). Thus amino acids 1–10 are required for Pto signalling, regardless of the presence of AvrPto or the CGF mutation. Roles for amino acids 20–30 could not be distinguished in these experiments because of the null phenotypes of pto[N-10] molecules.

Amino-terminal residues influence ligand-binding and kinase activities of Pto

To investigate specific roles for amino-terminal residues in Pto function, we assayed the ability of the deletion mutants to interact with AvrPto or AvrPtoB in yeast. Co-expression of wild-type Pto fused to the GAL4 DNA-binding domain (BD), with AvrPto or AvrPtoB expressed as GAL4 transcriptional activation domain (AD) fusions, allowed yeast to grow on selective media (Wu *et al.*, 2004; Figure 2a). Co-expression of BD-pto[N-10] with AD-AvrPto or with AD-AvrPtoB restored yeast growth similarly to the wild-type control. Interaction between the BD-pto[N-20] fusion and AD-AvrPto was reduced in comparison with the wild type, as indicated by slower growth, suggesting a contribution of residues 11–20 to interaction with AvrPto. Reduced growth was not observed for co-expression of BD-pto[N-20] and AD-AvrPtoB. Yeast co-expressing BD-pto[N-30] and AD-AvrPto or AD-AvrPtoB did not grow, indicating that these proteins were not able to interact. Western blotting with specific antisera confirmed accumulation of BD-pto[N-30] and other BD fusion proteins, so the lack of growth was not due to instability of the fusion protein (Figure 2b). These data demonstrate that residues 20–30 of Pto are required for ligand interaction in yeast. Furthermore, residues 11–20 appear to contribute to the interaction with AvrPto, but not AvrPtoB.

The data presented above preclude that the signalling deficiency of pto[N-10] is in interaction with AvrPto or AvrPtoB. Pto requires its intrinsic kinase activity for adoption of the active form after stimulation by AvrPto, although kinase activity is dispensable thereafter for signalling (Rathjen *et al.*, 1999; Salmeron *et al.*, 1994; Wu *et al.*, 2004). To test the phosphorylation ability of truncated molecules, we constructed genetic fusions of Pto derivatives with the glutathione-*S*-transferase (GST) protein. Fusion constructs were expressed in *Escherichia coli*, purified, and subjected to an *in vitro* kinase assay with Ptil^{K96N} as the substrate (Wu *et al.*, 2004; Zhou *et al.*, 1995).

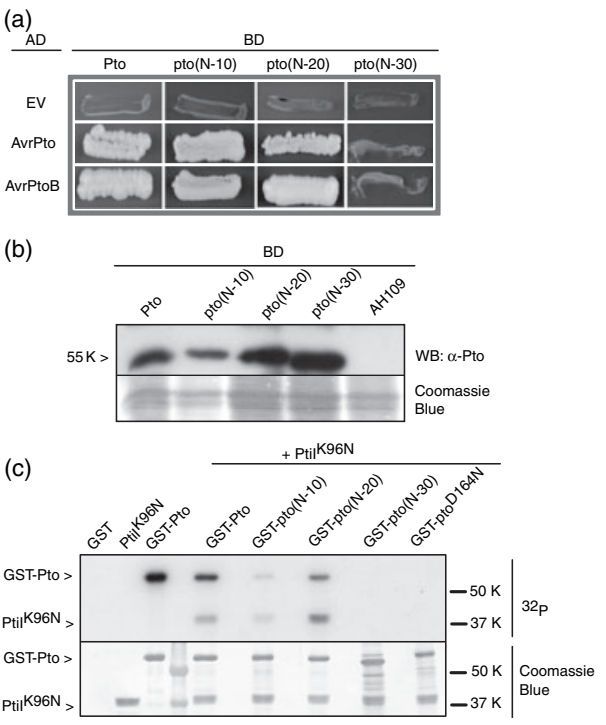

Figure 2. Amino-terminal residues influence ligand-binding and kinase activities of Pto.
(a) Interaction of most *N*-terminal deletion mutants with AvrPto or AvrPtoB in yeast two-hybrid. Growth represents a positive interaction; absence indicates a lack of interaction.
(b) Accumulation of all mutant proteins in yeast. Pto proteins were expressed as *C*-terminal fusions with the GAL4 DNA-binding domain. AH109 indicates protein extracted from non-transformed yeast. Coomassie Blue staining of the Western blot membrane (bottom panel) confirmed similar loading.
(c) Kinase activity of *N*-terminal deletion pto mutants. Mutant proteins were expressed as GST fusions and assayed for the ability to autophosphorylate or transphosphorylate *in vitro*. Radiolabelled species were detected by autoradiography after SDS-PAGE. The positions of GST-Pto fusion proteins and the cleaved Pti1^{K96N} fusion substrate are indicated. Coomassie Blue staining of the membrane used for autoradiography confirmed equivalent loading (bottom panel).

Autoradiography of the proteins after SDS-PAGE revealed an autophosphorylation band corresponding to the expected GST-Pto size of approximately 60 K, and transphosphorylation of Ptil^{K96N} at approximately 40 K (Figure 2c). Conversely, the kinase-deficient mutant GST-pto^{D164N} lacked both activities. Both GST-pto[N-10] and GST-pto[N-20] were active kinases, although their activities were reduced relative to GST-Pto. Strikingly, GST-pto[N-10] was less active than GST-pto[N-20] (Figure 2c). In contrast, GST-pto[N-30] lacked detectable autophosphorylation in this assay, and did not phosphorylate the Ptil^{K96N} substrate protein. Coomassie Blue staining of the gel confirmed purity and equivalent loading of the GST fusion and substrate proteins (Figure 2c). These data show that the inability of pto[N-10] or pto[N-20] to transduce a signal cannot be attributed to lack of kinase activity. Deletion of

© 2005 The Authors
Journal compilation © 2005 Blackwell Publishing Ltd,

residues N1–30 abolished detectable activity in any of the assays described here, and both the pto[N-30] and pto[N-30]^{L205D} mutants were excluded from subsequent experiments.

A heterologous N-*terminus complements the Pto* N-*myristoylation motif*

Pto residues 1–10 constitute a consensus myristoylation motif, which was dispensable for disease resistance in tomato (Loh *et al.*, 1998; Martin *et al.*, 1993). To investigate a role for this motif in Pto function in *N. benthamiana*, we exchanged residues 1–10 for a heterologous *N*-myristoylation motif encoded by the first 10 amino acids of *A. thaliana* calcium-dependent protein kinase 3 (AtCPK3; At4g23650; Figure 3a). This sequence, referred to here as M_{CPK3}, was fused genetically to deletions of both wild-type and CGF forms of *Pto*, and the mutants expressed as fusions with the FLAG epitope as described above. Transient expression of either wild-type *Pto*, M_{CPK3}-*pto*[*N-10*] or M_{CPK3}-*pto*[*N-20*] in *N. benthamiana* did not elicit the HR in the absence of *avrPto* induction (Figure 3b). Co-expression of *avrPto* induced the HR within the area of infiltration in the wild-type *Pto* control, and for both M_{CPK3}-*pto*[*N-10*] and M_{CPK3}-*pto*[*N-20*]. Expression of M_{CPK3}-*pto*[*N-10*]^{L205D} or M_{CPK3}-*pto*[*N-10*]^{L205D} in wild-type *N. benthamiana* induced the HR within 48 h, similar to *pto*^{L205D}. Western blotting confirmed that protein accumulated from the expression of all mutant genes (Figure 3c). Thus the M_{CPK3} sequence complemented the AvrPto-dependent and CGF-signalling phenotypes of pto[N-10] and pto[N-20], consistent with a role in *N*-myristoylation.

To test whether the mutants described above activated the cognate signalling pathway, virus-induced gene silencing (VIGS) was used to silence an *N. benthamiana Prf* (*NbPrf*) homologue in *N. benthamiana*. Virus-induced gene silencing of the *NbPrf* gene specifically compromised disease resistance to *P. syringae* pv. *tabaci* expressing *avrPto* and abolished the *Pto*-dependent HR (Lu *et al.*, 2003; Wu *et al.*, 2004). *Nicotiana benthamiana* plants silenced for *NbPrf* or the empty tobacco rattle virus (TRV) vector (Ratcliff *et al.*, 2001), were infiltrated with *Agrobacterium* strains containing M_{CPK3}-*pto*[*N-10*], M_{CPK3}-*pto*[*N-10*]^{L205D}, or the positive control *Pto* with *avrPto*. Co-expression of *Pto* with *avrPto* did not induce the HR in *NbPrf* silenced plants, but the HR was confluent in 5 days in the empty vector control (Figure 3d). Thus the loss of HR was due to the silencing of *NbPrf* and not to secondary effects of VIGS. Similarly, the *avrPto*-dependent HR of M_{CPK3}-*pto*[*N-10*] and the CGF phenotype of M_{CPK3}-*pto*[*N-10*]^{L205D} were absent in *N. benthamiana* tissue silenced for *NbPrf*, but induced in the empty vector control in 5 or 3 days, respectively (Figure 3d). These data are consistent with activation of the native signalling pathway by M_{CPK3} fusion mutants.

Pto-mediated signal transduction in N. benthamiana *is dependent on Gly-2*

Conjugation of myristate to proteins is absolutely dependent on a glycine residue at position 2. To test the role of Gly-2 in Pto signalling, we mutated the base triplet encoding Gly-2 to specify Ala (G2A), in both wild-type and CGF backgrounds of Pto-FLAG. These molecules were expressed with or without *avrPto*, respectively, in wild-type *N. benthamiana*. Co-expression of wild-type *Pto* with *avrPto* induced the HR within the infiltrated area in 4 days (Figure 4a). Conversely, co-expression of *pto*^{G2A} and *avrPto* never resulted in tissue necrosis. Similar results were observed for the CGF mutant pto^{L205D}. Expression of *pto*^{L205D} induced cell death within 3 days, whereas the double mutant *pto*$^{G2A:L205D}$ was completely inactive (Figure 4a). Protein accumulation from expression of both G2A mutants was confirmed by Western blotting (Figure 4b). Therefore the lack of HR was not due to the absence of the mutant proteins, as these accumulated to a higher level than wild-type Pto. Thus Gly-2 is absolutely required for Pto signalling in *N. benthamiana*, consistent with the requirement for an *N*-myristoylation site.

The N-*myristoylation motif of Pto is functional*

AvrPto requires the myristoylation site Gly-2 for avirulence activity and plasma membrane association (Shan *et al.*, 2000). We asked if Pto amino acids 1–10 (M_{Pto}) could substitute for the AvrPto myristoylation motif (Figure 5a). We made a construct encoding the M_{Pto} sequence fused to codons 11–164 of AvrPto, designated M_{Pto}-*avrPto*. Expression of M_{Pto}-*avrPto* in the absence of Pto did not induce the HR, similarly to wild-type *avrPto*. Transient co-expression of M_{Pto}-*avrPto* and *Pto* in *N. benthamiana* leaves induced the HR within the area of infiltration in 3 days (Figure 5b). The phenotype was indistinguishable from stimulation of Pto by wild-type AvrPto. Thus residues 1–10 of Pto complemented the *N*-myristoylation motif of AvrPto. AvrPto expressed *in planta* is associated with the plasma membrane dependent on Gly-2 (Shan *et al.*, 2000). To test whether the Pto *N*-myristoylation motif confers membrane association to AvrPto, we conducted subcellular fractionation experiments on extracts from tissue transiently expressing M_{Pto}-*avrPto*. An approximately 18-K band corresponding to the predicted size of AvrPto was detected using specific polyclonal antisera in total cell extracts of tissue expressing either *avrPto* or M_{Pto}-*avrPto* (Figure 5c). Fractionation of these extracts with ultra-speed centrifugation showed that the AvrPto and M_{Pto}-avrPto signal was predominantly in the insoluble fraction, corresponding to membranous particles. Traces of AvrPto were also detected in the soluble fraction (Figure 5c).

© 2005 The Authors
Journal compilation © 2005 Blackwell Publishing Ltd,

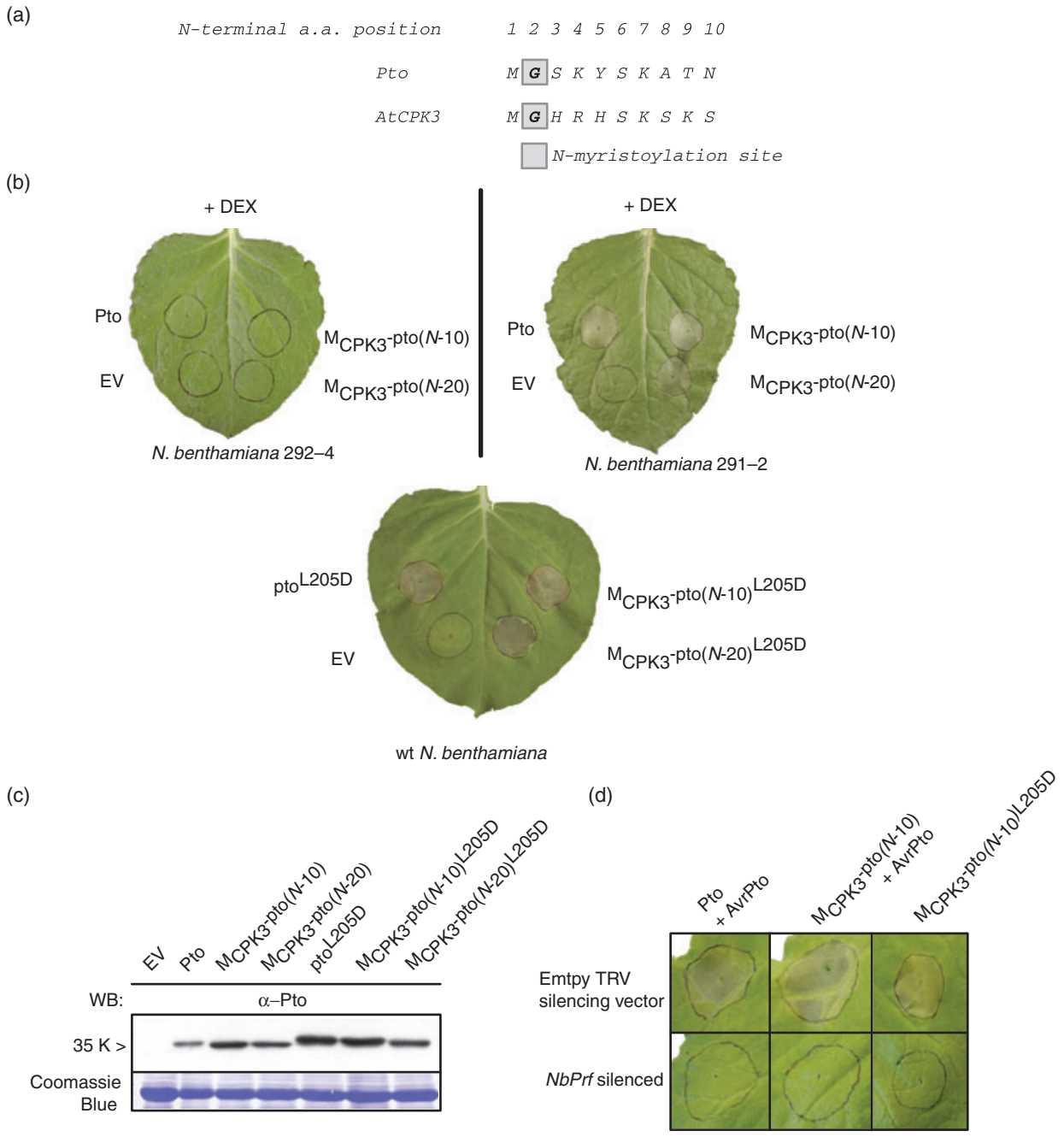

Figure 3. A heterologous *N*-terminus complements the Pto *N*-myristoylation motif.
(a) Alignment of the *N*-myristoylation motifs of Pto (Martin *et al.*, 1993) and AtCPK3 (At4g23650).
(b) Transient expression of the *N*-terminal deletion mutants of Pto fused to the M_{CPK3} sequence. *Nicotiana benthamiana* leaves were infiltrated with *Agrobacterium tumefaciens* containing each construct as indicated. Expression of avrPto was induced in line 291–2 upon treatment with dexamethasone (DEX). *Nicotiana benthamiana* line 292–4 harbours an empty DEX-inducible element (Chang *et al.*, 2002). Upper leaves are shown 4 days after infiltration with *Agrobacterium* containing each construct, as indicated; bottom leaf, 3 days after infiltration.
(c) Accumulation of all mutant proteins *in planta*. Total protein was extracted from leaves transiently expressing each construct and blotted against polyclonal anti-Pto antisera after SDS-PAGE. Equivalent loadings were confirmed by Coomassie Blue staining of the membrane (bottom panel).
(d) The *NbPrf* gene is required for cell death induced by the M_{CPK3} fusion mutants. Top row, *N. benthamiana* silenced for the empty virus-induced gene silencing vector; bottom row, *N. benthamiana* silenced for the *NbPrf* gene. Topmost leaves were infiltrated with each *Agrobacterium* culture as indicated, 4 weeks after inoculation with the TRV-silencing vector.

© 2005 The Authors
Journal compilation © 2005 Blackwell Publishing Ltd,

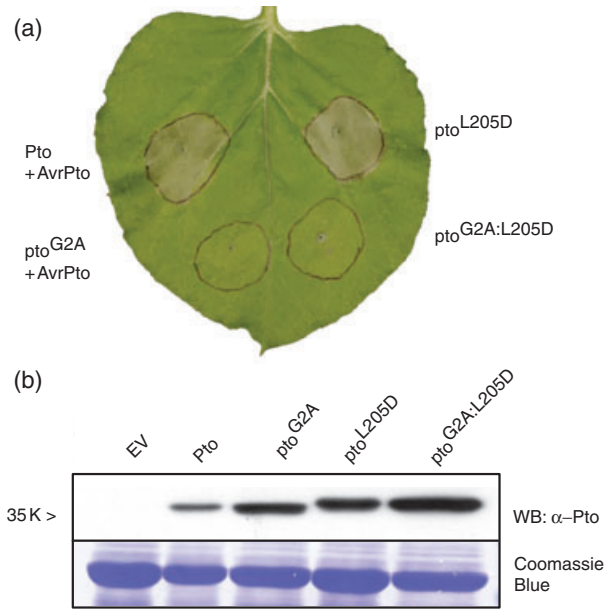

Figure 4. Pto requires the Gly-2 residue for signalling in *Nicotiana benthamiana*.
(a) Transient expression of G2A mutants in the presence or absence of AvrPto. *Nicotiana benthamiana* leaves were infiltrated with *Agrobacterium* containing each construct as indicated. For co-expression of *avrPto*, bacterial cultures were mixed in a 1:1 ratio. The area of infiltration was outlined with a marker pen. Leaf shown 4 days after infiltration, and represents more than three independent repeats.
(b) Accumulation of G2A mutant proteins *in planta*. Total protein was extracted from leaves and blotted against anti-Pto antisera. Equivalent loadings were confirmed by Coomassie Blue staining of the membrane (bottom panel).

Qualitatively more M_{Pto}-avrPto signal could be detected in the soluble fraction than wild-type AvrPto, and this pattern was observed consistently in all experiments. Thus the Pto *N*-myristoylation motif may afford weaker membrane association than the wild-type AvrPto sequence.

The above data suggest that *Pto* encodes a functional *N*-myristoylation motif. We used an *in vivo* myristoylation assay to test this hypothesis directly. Pto-FLAG or pto^{G2A}-FLAG were expressed transiently in *N. benthamiana* leaves using *Agrobacterium* as described. Leaf patches expressing each protein were infiltrated with a solution of tritiated myristate for *in vivo* labelling of proteins. Wild-type Pto and pto^{G2A} were recovered from extracts by immunoprecipitation using anti-FLAG beads. Accumulation of each mutant protein was confirmed by SDS-PAGE followed by Western blotting with the anti-FLAG antibody. The pto^{G2A} mutant accumulated to a qualitatively higher level than Pto (Figure 5d). The Western blot membrane containing the immunoprecipitated proteins was exposed on a phosphorimager plate to detect tritiated species. Phosphorimager autoradiography reproducibly showed a band corresponding to wild-type Pto, consistent with incorporation of myristate (Figure 5d). By comparison, pto^{G2A} showed absent or vastly reduced incorporation of tritium. These data are consistent with conjugation of myristate to the Gly-2 residue of Pto *in vivo*.

Pto is a soluble protein and resides in the cytoplasm

The requirement for *N*-myristoylation suggests that Pto could be targeted to a cellular membrane. To test this, we used subcellular fractionation to determine the localization of Pto. In these experiments, *Pto* was expressed from its native promoter (Pro_{Pto}) because overexpression from the CaMV *35S* promoter resulted in non-specific localization in both membrane and soluble fractions (data not shown). The *Pto* promoter has not been characterized, so a 2.2-kb fragment of genomic DNA upstream of, and contiguous with, the Pto ATG start codon was cloned to ensure transcriptional activity. Pro_{Pto}-*Pto* was fused *N*-terminally to a sequence encoding three tandem hemagglutinin (HA) epitopes in a binary vector, to allow transient expression *in planta* as described above. The Pro_{Pto}-*Pto-3HA* construct induced the HR in *N. benthamiana* upon co-expression with AvrPto, demonstrating that Pto-3HA accumulated and was functional (data not shown). A total protein extract containing Pto-3HA expressed from the genomic promoter was subjected to subcellular fractionation by ultracentrifugation. Equal volumes of the total protein extract, the supernatant, and the resuspended microsomal pellet were analysed with the anti-HA antibody for the presence of Pto. A band of approximately 40 K corresponding to Pto-3HA was detected in the total protein extract, but was absent from the empty vector control (Figure 6a). A band of similar intensity compared with the total extract was detected in the soluble fraction. Conversely, only trace amounts of Pto were observed in the microsomal fraction. These data indicate that Pto is a soluble protein.

To determine whether the faint Pto band in the microsomal fraction was due to *N*-myristoylation of Pto, we constructed the mutant molecule Pro_{Pto}-*pto*^{G2A}*–3HA*. In contrast to Pro_{Pto}-*Pto-3HA*, the Pro_{Pto}-*pto*^{G2A}*-3HA* construct did not mount the HR in *N. benthamiana* upon co-expression with *avrPto* (data not shown). However, pto^{G2A}-3HA accumulated when expressed from the genomic promoter (Figure 6b). A total protein extract containing pto^{G2A}-3HA was subjected to subcellular fractionation and analysed with the anti-HA antibody, as described for wild-type Pto. Bands of nearly identical intensity corresponding to pto^{G2A}-3HA were detected in the total protein extract and in the soluble fraction (Figure 6b). Conversely, only trace amounts of pto^{G2A} were observed in the microsomal fraction. Thus the fractionation pattern observed for wild-type Pto and pto^{G2A} is identical. These data indicate that *N*-myristoylation does not account for the faint Pto band in the microsomes.

© 2005 The Authors
Journal compilation © 2005 Blackwell Publishing Ltd,

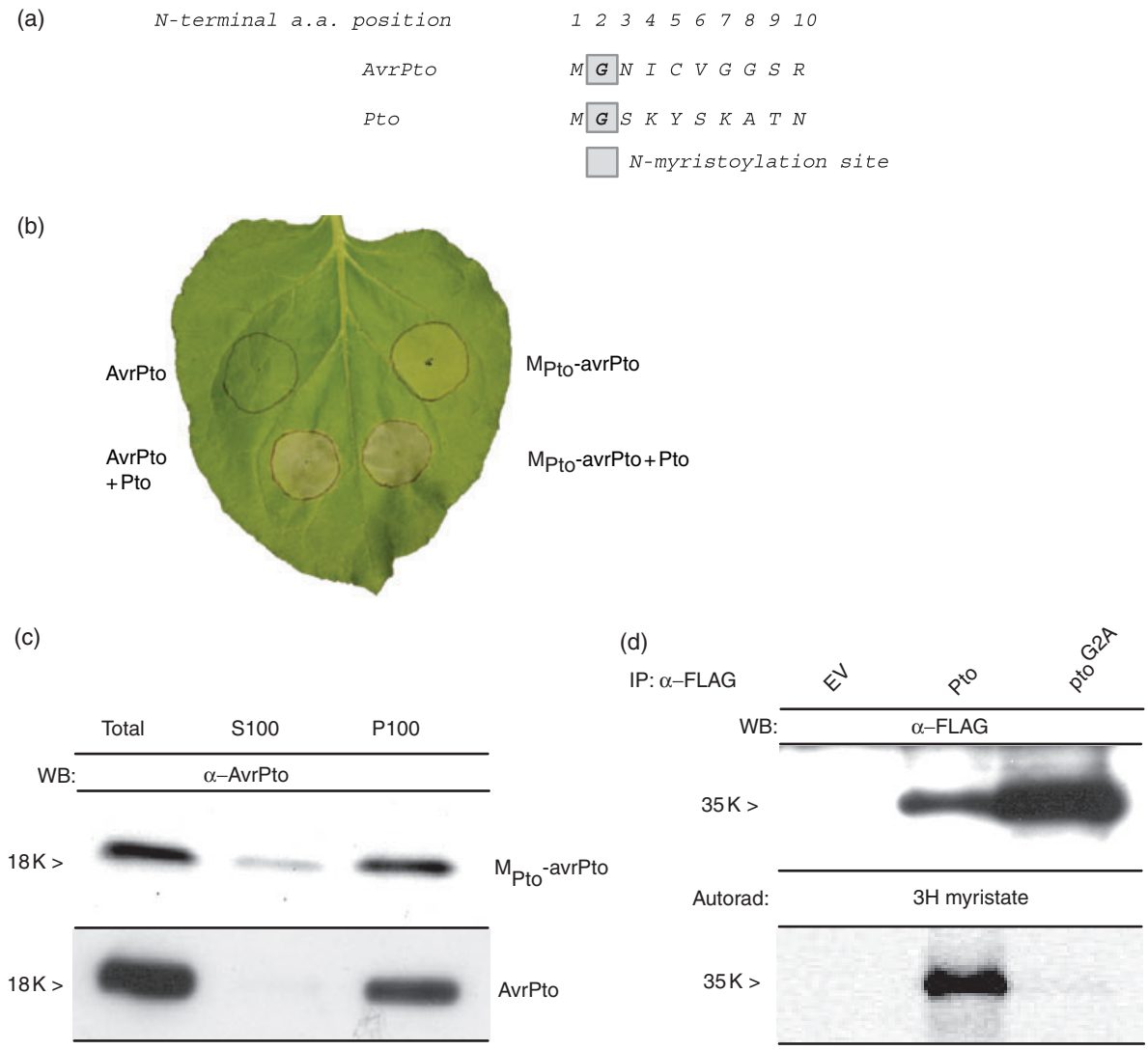

Figure 5. The *N*-myristoylation motif of Pto is functional.
(a) Alignment of the *N*-myristoylation motifs of AvrPto (Ronald *et al.*, 1992) and Pto (Martin *et al.*, 1993).
(b) Transient expression of *avrPto* fused to the M_{Pto} sequence results in the hypersensitive response in the presence of tomato *Pto*. The *Nicotiana benthamiana* leaf was infiltrated with *Agrobacterium* containing each construct as indicated. For co-expression of *Pto*, bacterial cultures were mixed in a 1:1 ratio. Leaf shown 4 days after infiltration.
(c) Protein extracts from *N. benthamiana* leaf tissue transiently overexpressing *avrPto* or *M_{Pto}-avrPto* were fractionated by ultracentrifugation. A volume of the total extract corresponding to 25 μg protein, and equal volumes of the supernatant (S100) and microsome (P100) fractions, were immunoblotted against polyclonal anti-AvrPto antisera.
(d) Incorporation of tritiated myristate into Pto is Gly-2-dependent. *Nicotiana benthamiana* leaves were inoculated with *Agrobacterium* carrying FLAG epitope-tagged constructs of Pto, pto^{G2A}, or the empty vector control (EV). After 24 h, an aqueous solution of tritiated myristic acid was infiltrated in the area of protein expression. Total protein extracts were prepared after a further 24 h, and the tagged proteins recovered by immunoprecipitation with anti-FLAG agarose beads. Similar amounts of each construct were blotted against the anti-FLAG antibody. The same membrane was used for detection of the tritium signal on a phosphorimager plate.

To investigate the *in vivo* localization of Pto, we used confocal laser microscopy to detect Pto fused to the green fluorescent protein (Pto-GFP). All GFP constructs described here were driven by the CaMV 35S promoter, because protein accumulation from the Pro_{Pto} promoter was insufficient for GFP detection (data not shown). Localization controls included the unfused *GFP* gene, *avrPto-GFP*, and *pto^{G2A}-GFP*. All GFP fusion constructs were transiently expressed *in planta* to confirm function and accumulation of the fusion proteins (data not shown). Pto was functional and stable upon *C*-terminal fusion to GFP. Wild-type *N. benthamiana* cell-suspension cultures were transformed with *Agrobacterium* for transient expression of the GFP constructs, and analysed with confocal laser microscopy.

© 2005 The Authors

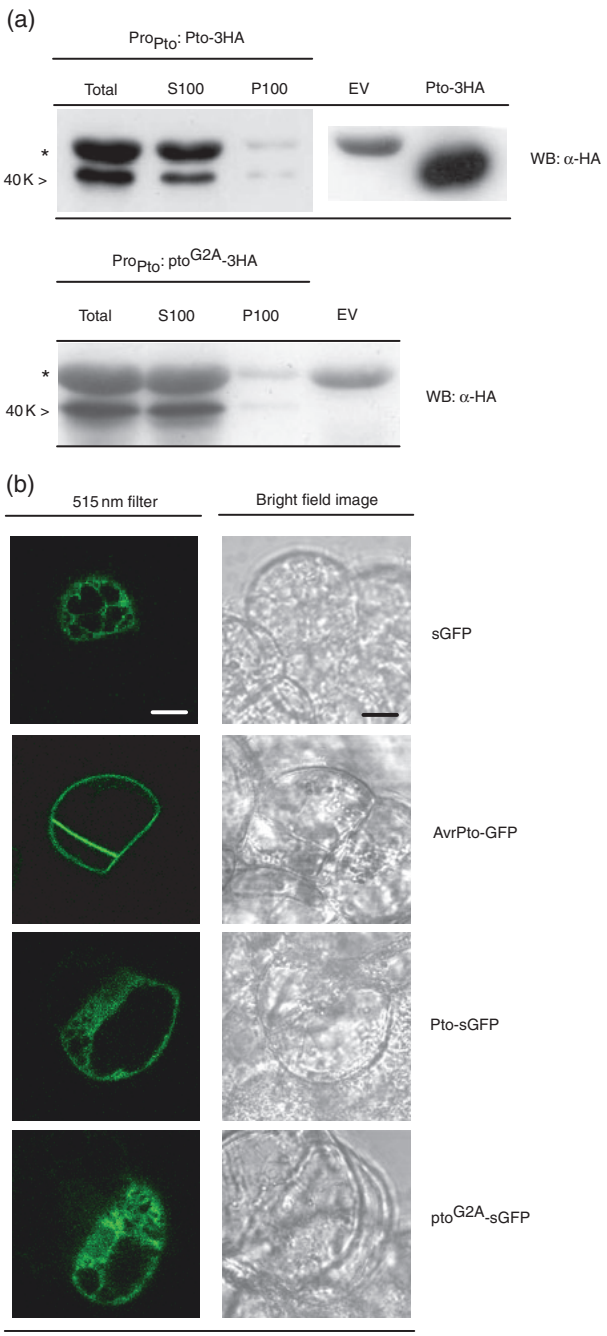

Figure 6. Pto is soluble and resides in the cytoplasm.
(a) Subcellular fractionation of *Nicotiana benthamiana* leaf tissue transiently expressing wild-type Pto-3HA or myristoylation-deficient pto^{G2A}-3HA from the genomic Pto promoter (Pro$_{Pto}$). An asterisk indicates a non-specific band. EV, empty vector control. Pto-3HA corresponds to an immunoprecipitated sample, hence the absence of the cross-reacting band. A volume of the total extract corresponding to 25 μg protein, and equal volumes of the supernatant (S100) and microsome (P100) fractions, were immunoblotted against polyclonal anti-hemagglutinin antisera.
(b) Transient overexpression of GFP fusions in *N. benthamiana* cell cultures. Single-cell transformants were analysed 3 days after *Agrobacterium*-mediated transformation. Each confocal image consists of 10 stacked sections. Bar, 20 μm.

The fluorescent signal from unfused GFP was detected throughout the cell (Figure 6b). In most cells, the signal was concentrated in the nucleus, as is typical for GFP (data not shown). In contrast, *avrPto-GFP* was detected at the periphery of the cell but not intracellularly (Figure 6b). This is consistent with plasma membrane association of AvrPto as reported by Shan *et al.* (2000). The wild-type Pto-GFP signal was characteristically strong throughout the cell, resulting in bright fluorescence (Figure 6b). The signal was not concentrated at the cell periphery, as would be expected for plasma membrane localization (Murase *et al.*, 2004). Similar to Pto-GFP, the pto^{G2A}-GFP signal was diffused throughout the cell (Figure 6b). Taken together, the data are consistent with Pto as a soluble cytoplasmic protein, irrespective of myristoylation status at residue 2.

AvrPtoB is a soluble protein

Localization of Pto within the cytoplasm is puzzling, given that AvrPto is a plasma-membrane protein (Shan *et al.*, 2000). In contrast, AvrPtoB was suggested to be a soluble protein (Kim *et al.*, 2002). To test the solubility of AvrPtoB, *avrPtoB-HA* was transiently expressed from the 35S promoter in wild-type *N. benthamiana*, as described previously for AvrPto. A band of approximately 70 K corresponding to full-length AvrPtoB-HA was detected in the total protein extract (Figure 7). A band of the same size was also observed with specific detection of AvrPtoB-FLAG (data not shown). Similar amounts of AvrPtoB-HA were detected in the total extract and soluble fraction, respectively. Conversely, only trace amounts of AvrPtoB were observed in the microsomal fraction. These data indicate that AvrPtoB is a soluble protein. In addition to the full-length AvrPtoB protein, several faster-migrating bands were observed that cross-reacted with the specific antisera, but were absent from empty vector controls (data not shown). These may represent fragments of AvrPtoB, although their genesis is unknown. None of these novel bands associated with the membranous

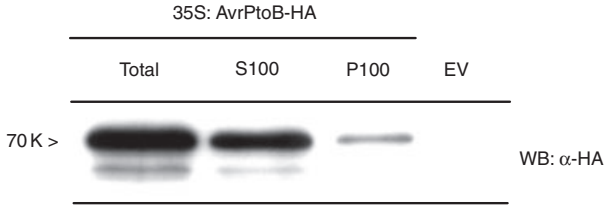

Figure 7. AvrPtoB is a soluble protein.
Subcellular fractionation of *Nicotiana benthamiana* leaf tissue transiently expressing AvrPtoB from the CaMV 35S promoter (35S). EV, empty vector control. A volume of the total extract corresponding to 25 μg protein, and equal volumes of the supernatant (S100) and microsome (P100) fractions, were immunoblotted against polyclonal anti-HA antisera.

© 2005 The Authors
Journal compilation © 2005 Blackwell Publishing Ltd,

fraction during these experiments. These fragments await further characterization.

Discussion

The data presented here show that the *N*-terminal non-kinase domain residues are important for Pto function. Deletions in this region abolished Pto-mediated signalling in *N. benthamiana*. The *N*-terminus contributed to both AvrPto-binding and phosphorylation activities of Pto. Further observations strongly suggest a role for *N*-myristoylation in Pto function. A heterologous *N*-myristoylation motif complemented signalling by *N*-terminal deletion mutants of Pto. In contrast to Loh *et al.* (1998), we found a strict requirement for Gly-2 in Pto function. The Pto *N*-terminus functionally complemented the *N*-fatty acylation motif of AvrPto for avirulence function and membrane association. Finally, the Gly-2 residue was required for *in vivo* myristoylation of Pto. Taken together, the data are consistent with multiple roles for the *N*-terminus in control of signalling by Pto.

A role for the Pto N*-terminus in signalling*

Most investigations of structure–function relationships in the Pto protein have focused on the role of the kinase domain. The protein kinase domain is an intricately folded unit which brings subdomains required for ATP and protein substrate binding into proximity and precise orientation for catalytic phosphotransfer. In addition, a patch of 21 surface residues overlapping the Pto kinase domain provides the major determinant of AvrPto and AvrPtoB binding. Therefore the ability of mutant Pto proteins to phosphorylate or to interact with the respective Avr proteins provides a sensitive, if indirect, measure of tertiary conformation of the kinase domain. On this basis, the tertiary structure of pto[N-10] and pto[N-20] appeared to be preserved as both mutants retained AvrPto-binding and kinase capabilities, although these were not the same as the wild-type controls. However, *pto*[*N-10*] and *pto*[*N-20*] were unable to induce the *avrPto*-dependent HR upon expression in *N. benthamiana*. The lack of phenotype upon *in planta* expression of these mutants cannot be explained by the results of the *in vitro* experiments. The *N*-terminus must therefore play a role in signalling to the HR. This is supported by the lack of an *in planta* phenotype of *N*-terminal deletion mutants of pto^{L205D}, which mimics Pto in a terminally active state because it signals independently of ligands or kinase activity (Wu *et al.*, 2004). The *in vitro* kinase activity and Avr-binding phenotypes of pto[N-10] and pto[N-20] suggests that the Pto *N*-terminus is primarily involved in signal transduction rather than in perception.

A likely explanation for the requirement of the *N*-terminal 10 residues in Pto signalling is the presence of an *N*-myristoylation motif. Accordingly, the heterologous M_{CPK3} sequence functionally complemented both wild-type Pto and pto^{L205D} lacking either 10 or 20 *N*-terminal amino acids. *Pto* and *AtCPK3* both encode consensus myristoylation sites including the essential Gly-2 residue, while lacking residues at other positions that are non-permissible for *N*-myristoylation (Boisson *et al.*, 2003; Maurer-Stroh *et al.*, 2002). The consensus *N*-myristoylation motif is thus conserved between the two sequences, and peptides corresponding to either sequence were *N*-myristoylated *in vitro* (Qi *et al.*, 2000). Residues other than Gly-2 are less strictly conserved between M_{Pto} and M_{CPK3}, but these differences are apparently tolerated for Pto function.

Other roles for the Pto N*-terminus*

The *N*-terminal residues 11–20 are broadly conserved among the predicted Pth proteins, suggesting a general role for these residues among the family members (Chang *et al.*, 2002). Consistent with this observation, residues 11–20 contributed qualitatively to AvrPto binding in yeast, but were dispensable for the interaction with AvrPtoB. Unexpectedly, deletions of *N*-terminal amino acids had an impact on Pto kinase activity. The pto[N-10] mutant showed reduced auto- and transphosphorylation activity relative to wild-type Pto, but this was restored by further removal of amino acids 11–20. Thus *N*-terminal residues exert both positive and negative influences on kinase activity. These data are striking because they appear to link the *N*-terminal residues directly with the kinase domain, in particular the catalytic cleft of Pto. Residues 1–20 are positioned well outside the conserved kinase domain, which begins at residue 41 (Hanks and Hunter, 1995). We therefore suggest the possibility that the *N*-terminal residues are folded back into the kinase domain, where they could physically influence events (e.g. substrate binding) in the catalytic cleft of the enzyme. This model awaits more detailed investigation, but the reduced ability of pto[N-20] to interact with AvrPto is consistent with this idea, because the catalytic cleft is overlapped by the principal site of Avr interaction. However, we note that AvrPtoB did not show altered interactions with pto[N-10] or pto[N-20], which could be inconsistent with the folding model proposed above, or further evidence of divergent requirements for interaction of Pto with AvrPto and AvrPtoB. Deletions of 30 amino acids destroyed all known activities of Pto or pto^{L205D}, and we speculate that these proteins are misfolded. Sessa *et al.* (2000) showed similar data for the protein pto^{T38A}, which was mutated in a site of *in vitro* phosphorylation. Thus residues between 20 and 40 may contribute to Pto structure and stability. In summary, the data are consistent with the contribution of the Pto *N*-terminus to multiple activities characteristic of Pto.

© 2005 The Authors
Journal compilation © 2005 Blackwell Publishing Ltd,

Despite this, the M_{CPK3} sequence complemented both Pto amino acids *N*1–10 and *N*1–20. Moreover, the AvrPto-dependent HR phenotypes of M_{CPK3} fusions lacking either 10 or 20 *N*-terminal Pto amino acids were indistinguishable (Figure 3). Thus an absolute requirement for residues *N*10–20 in Pto-mediated signalling was not detected in these experiments. The data afford at least two possible explanations. First, residues 1–10 of both Pto and CPK3 constitute related functional myristoylation motifs, so it is possible that the CPK3 motif effectively complements Pto *N*1–10 for AvrPto interaction and kinase capabilities. We did not assay these activities of the CPK3 fusion proteins directly, so this hypothesis cannot be excluded. Second, all the *in planta* data presented here were derived from 35S promoter overexpression, which may have obscured quantitative phenotypes. Further progress on the exact orientation of the Pto *N*-terminus *vis-à-vis* the catalytic cleft, and the implications for kinase activity and Avr recognition, await more extensive experimentation.

A role for N-*myristoylation in Pto function*

Our data demonstrate that induction of the AvrPto-dependent HR and the CGF phenotype was abolished by the G2A mutation within the consensus *N*-myristoylation motif. This further indicates that Pto encodes a functional *N*-myristoylation site. Consistent with this notion, fusion of the Pto *N*-myristoylation motif to residues 11–164 of AvrPto complemented the avirulence activity of this protein. Furthermore, M_{Pto}-avrPto was detected primarily in the microsomal fraction in subcellular fractionation experiments, similarly to wild-type AvrPto. This result is significant because Shan *et al.* (2000) demonstrated that attachment of AvrPto to the plasma membrane depends on the Gly-2 residue. Thus the M_{Pto} sequence conferred membrane association to AvrPto. The AvrPto myristoylation motif contains a Cys residue at position 5 (Cys-5), which is likely to be modified by palmitate, a 16-C saturated fatty acid moiety. *N*-myristoylation in conjunction with palmitoylation confers stable membrane anchoring to modified proteins. In contrast, modification by *N*-myristoylation alone provides weak membrane-association characteristics (Resh, 1999). Therefore the reduced membrane association provided to AvrPto by the M_{Pto} sequence can be explained by the lack of a palmitoylable Cys residue. Despite these differences, the Pto-dependent HRs induced by wild-type AvrPto or M_{Pto}-avrPto were indistinguishable. This may simply be the result of complementation of phenotype by overexpression. Alternatively, the avirulence activity of AvrPto may require *N*-fatty acylation, but not membrane localization. This idea seems unlikely, because severe overexpression of $avrPto^{G2A}$ from the DEX-inducible promoter induced the Pto-dependent HR (M.E. Sierla and J.P.R., unpublished data). Similarly, overexpression of myristoylation-deficient derivatives of three *Pst* effector proteins complemented their respective avirulence phenotypes (Nimchuk *et al.*, 2000). Therefore the requirement for specific membrane-targeting signals can be overcome by ubiquitous localization as a result of enhanced protein accumulation.

We demonstrated that Pto incorporated tritiated myristate *in vivo*, dependent on the Gly-2 residue. Thus Pto is a substrate for *N*-myristoyl transferase of *N. benthamiana*. This corroborated the requirement of Gly-2 for the AvrPto-dependent and CGF phenotypes of Pto. The data are therefore consistent with a requirement for *N*-myristoylation in Pto-mediated signal transduction leading to defence responses. Conversely, Loh *et al.* (1998) found that the Gly-2 to Ala mutation did not compromise *Pto*-mediated disease resistance. This conclusion was based on the absence of symptoms of bacterial speck disease on transgenic tomato lines expressing $35S{:}pto^{G2A}$, although bacterial growth was not quantified in these experiments. Other data predict a requirement for *N*-myristoylation in Pto function, in agreement with the findings presented here. The *N*-myristoylation motif is conserved among Pto and the Pth family members (Chang *et al.*, 2002; Martin *et al.*, 1993; Rommens *et al.*, 1995). Accordingly, the Pto homologue Fen required Gly-2 for function, and its *N*-terminus was myristoylated in an *in vitro* assay (Qi *et al.*, 2000; Rommens *et al.*, 1995). Thus *Pto* and *Fen* encode identical *N*-myristoylation motifs which are required for signalling. The discrepancy between the observations presented here and those of Loh *et al.* (1998) could potentially be explained by putative genetic differences between *N. benthamiana* and tomato. However, other workers have reported that introduction of the G2A mutation abolished ligand-independent signalling by Pto in transgenic tomato plants (Pedley and Martin, 2003).

The reason for the loss of function of pto^{G2A} and $pto^{G2A:L205D}$ in *N. benthamiana* is unclear, but it is evidently the consequence of elimination of *N*-myristoylation. It is conceivable that the myristoyl moiety targets Pto to the plasma membrane for perception of AvrPto, which becomes anchored to the plasma membrane after deposition in the plant cytoplasm (Shan *et al.*, 2000). However, Pto was not associated with the plasma membrane. Pto resided in the soluble fraction after ultracentrifugation, and localized throughout the cytoplasm *in vivo*, as demonstrated by confocal microscopy. Thus two independent methods show that Pto is a cytoplasmic protein. This suggests that perception of Avr proteins by Pto may occur in the cytoplasm. Consistent with this idea, AvrPtoB appeared to be a soluble protein (Figure 7) (Kim *et al.*, 2002). Thus Pto and AvrPtoB may interact in the cytoplasm. The distinct subcellular localizations of Pto and AvrPto conflict with their physical interaction in yeast. However, the current data do not indicate whether the localization of Pto is static, or where the interaction between AvrPto and Pto takes place. Potentially, Pto translocates to the cell periphery upon deposition

© 2005 The Authors
Journal compilation © 2005 Blackwell Publishing Ltd,

of AvrPto in the plant cell. This question remains to be addressed.

The localization of pto^{G2A} was indistinguishable from wild-type Pto in cell fractionation and confocal microscopy experiments. Thus the *N*-myristoyl moiety did not contribute to subcellular localization *in vivo*. Accordingly, overexpression of pto^{G2A} or pto$^{G2A:L205D}$ did not complement the G2A mutation, as would be expected if the protein were mislocalized, despite high levels of accumulation of each mutant protein. We therefore suggest that the *N*-myristoyl moiety of Pto plays an alternative role to membrane localization. The requirement for the Gly-2 residue in pto^{L205D} suggests a function for *N*-myristoylation downstream of Avr perception and consequent kinase activity. We interpret this as indicating that the *N*-myristoyl moiety of Pto is involved in interactions with downstream signalling components. Alternatively, the *N*-myristoyl moiety is hidden inside Pto and is never exposed for interaction with other molecules. In this scenario, the *N*-myristoyl moiety would contribute solely to Pto autoregulation. In conclusion, elucidation of the role of the myristoylated *N*-terminus will provide important insights into mechanistic aspects of Pto activation.

A significant proportion of the *RPS5/RPS2* and the *RPP1* subfamilies of the NBS–LRR genes of *A. thaliana* encode consensus *N*-myristoylation motifs (Boisson *et al.*, 2003). In addition to these R genes, the PBS1 kinase, which is required for RPS5 function, also encodes an *N*-myristoylation motif (Boisson *et al.*, 2003; Swiderski and Innes, 2001). This suggests that *N*-myristoylation may be required for the function of several R proteins, although it is unknown whether these are myristoylated *in vivo*. Similarly, the *P. syringae* effector proteins AvrB, AvrRPM1 and AvrPphB were shown to encode functional eukaryotic *N*-myristoylation sites (Nimchuk *et al.*, 2000; Shan *et al.*, 2000). These effector proteins were modified with *N*-myristate upon transient expression *in planta*, and associated with the plasma membrane in an *N*-myristoylation-dependent manner. Importantly, the Gly-2 residue was required for avirulence of AvrPto, AvrB and AvrRPM1 in resistant plants, and for virulence of *P. syringae* in susceptible plants. These data illustrate the general importance of fatty acylation of R proteins and the potential functional implications of such modifications.

Methods

Cloning and expression of Pto mutants

Standard techniques for manipulating plasmids in *E. coli* strain DH5α were used (Sambrook *et al.*, 1989). PCR-based site-directed mutagenesis was performed as described (Horton *et al.*, 1989). All products contained *Nco*I and *Xba*I sites, and were cloned into pTOPO (Invitrogen, Carlsbad, CA, USA) before automated DNA sequencing (Applied Biosystems, Foster City, CA, USA). For *C*-terminal fusion of the FLAG tag, *N*-terminal mutants were subcloned in the sense orientation into the vector pSLJ4D4.1 (Jones *et al.*, 1992). The binary vector pTFS40 (Rathjen *et al.*, 1999) was used for expression of the cassette, containing the CaMV 35S promoter, gene and FLAG tag. Both strands of each mutant were sequenced after subcloning in pSLJ4D4.1 and in the binary vector. For construction of the GFP-fusions, the *sGFP^{S65T}* gene (Chiu *et al.*, 1996) was amplified from the pCAMBgfp vector (Sesma and Osbourn, 2004), and sequenced on both strands. The *sGFP^{S65T}* gene was inserted into pSLJ4D4.1. A linker sequence encoding a random coil, in single aa code ESGAKQGEKG (Case *et al.*, 2000), was inserted upstream of the *sGFP^{S65T}* gene. The linker was constituted by oligonucleotides, assembled during a temperature gradient of 60°C for 15 min, 37°C for 20 min, and 24°C for 15 min at a concentration of 25 μM each. A dilution of 1:100 of the assembled oligos was successfully ligated into pSLJ4D4.1 *sGFP^{S65T}*, and the orientation of the linker verified by PCR. Subsequently, the linker–*sGFP^{S65T}* fusion was inserted in the binary vector for *C*-terminal fusion to the CaMV *35S:Pto*R or *35S:pto^{G2A}*. The unfused sGFP^{S65T} control was directly transferred from the cassette excised from the pSLJ vector into the binary pTFS40. The a*vrPto* gene was fused to the *mGFP5* gene (Haseloff and Amos, 1995).

Recombinant binary vectors were transferred to *A. tumefaciens* strain C58C1 (pCH30) for transient expression *in planta*, and the presence of the binary vector was confirmed by PCR. Yeast two-hybrid analysis and protein expression in *E. coli* was performed as described elsewhere (Wu *et al.*, 2004).

Transient Agrobacterium*-mediated expression*

Agrobacterium tumefaciens strain C58C1 containing the binary plasmid of interest was grown as described for GV2260 by Wu *et al.* (2004). Use of *N. benthamiana* was as described elsewhere (Rathjen *et al.*, 1999; Scofield *et al.*, 1996). Plant growth conditions and transient expression were as described (Wu *et al.*, 2004). The transgenic 291–2 line harbours the DEX-inducible element (Aoyama and Chua, 1997). For expression of *avrPto* in *N. benthamiana* line 291–2 (Chang *et al.*, 2002), 30 μM dexamethasone (DEX; Sigma, St Louis, MO, USA) was applied with a paintbrush as an aqueous solution supplemented with 0.1% (v/v) Tween-20 (Sigma).

For transformation of *N. benthamiana* cell cultures, an *Agrobacterium* culture was prepared as described (Wu *et al.*, 2004). A volume of 6 ml 1-week-old subcultured cell suspensions of wild-type *N. benthamiana* was mixed with 150 μl bacterial suspension with an OD_{600} of 1.0–2.5. The mixture was incubated without shaking in the dark at 25°C for 3 days.

Labelling of Pto with tritiated myristate

An aliquot of a tritiated [9,10-^{3}H (*N*)] myristic acid stock solution in 100% ethanol (Perkin Elmer, Boston, MA, USA) was concentrated by heating for 30 min at 75°C. A volume of deionized water from a reverse-osmosis purification system was added to obtain a final concentration of 12.4 nmol ml^{-1} [9,10-^{3}H (*N*)] myristic acid (500 μCi ml^{-1}). For labelling with tritiated myristate *in vivo*, *Agrobacterium* containing FLAG-tagged wild-type Pto, pto^{G2A}, or the empty vector control was infiltrated in *N. benthamiana*. After 24 h of transient expression, 200 μl of the aqueous tritiated myristic acid solution was injected into each of the infiltrated areas. Prior to total protein extraction from each leaf disc infiltrated with tritiated myristate, incorporation of tritium was allowed for another 24 h. Subsequently, the tagged proteins were immunoprecipitated from the total protein extract using anti-FLAG-M2 agarose beads (Sigma).

© 2005 The Authors

FLAG immunoprecipitation

Leaf tissue transiently expressing each Pto mutant was pulverized in liquid nitrogen with a mortar and pestle. The homogenized leaf powder was mixed with extraction buffer containing 50 mM Tris–HCl pH 7.5, 150 mM NaCl, 2 mM DTT, 1 mM phenylmethylsulphonylfluoride (PMSF), 10% glycerol, 1.2% polyvinylpolypyrrolidone (PVPP) supplemented with a plant protease inhibitor cocktail (Sigma). The extract was centrifuged at 13 000 ***g*** for 30 min at 4°C, and filtered through 0.45 μm prior to immunoprecipitation. A volume of 40 μl equilibrated M2 anti-FLAG-agarose beads was added to 1 mg total protein. The mixture was incubated at 4°C for 1 h while mixing end-over-end. Subsequently the beads were washed with the extraction buffer, now lacking PMSF, protein inhibitors and PVPP. To determine incorporation of tritium, the beads were boiled in denaturing conditions for SDS-PAGE analysis.

Phosphorimager technology

The FUJI Film FLA5000 phosphorimager (FUJI, Tokyo, Japan) was used to scan the BAS TR2025 screen after 1 month of exposure with tritium. The image was analysed with FLA5000 ver. 1 software.

Subcellular fractionation

A total cell extract prepared in extraction buffer was cleared from complete cells and cell debris with a low-speed spin of 1500 ***g*** at 4°C. A subset of the cleared extract was subjected to an ultra-speed spin of 100 000 ***g*** in an Optima ultracentrifuge (Beckman-Coulter, Fullerton, CA, USA). After the ultra-speed spin, the supernatant was stored on ice and designated the S100 fraction. The microsomal pellet was rinsed once with 100 μl extraction buffer and resuspended in the original extract volume, which was designated the P100 fraction. A volume of the total cell extract corresponding to 25 μg protein, and equal volumes of the supernatant and the microsome fractions, were mixed with denaturing SDS-loading buffer for PAGE analysis. AvrPto proteins were resolved on Tris–Tricine buffered SDS-PAGE (Schagger and Von Jagow, 1987).

Fluorescent microscopy

Transient expression of GFP was verified with a Leica MZFLIII dissecting stereomicroscope (Leica Microsystems, Heidelberg, Germany) using the GFP-1 filter set. Images of single-cell transformants were taken with a DM RBE Leica confocal microscope with a TCS NT scanning head. GFP excitation was performed with an Argon laser emission of 488 nm and fluorescence filtered for 515 nm with magnification ×64. Images were processed with the LEICA CONFOCAL software version 2.00.

Other analysis

Virus-induced gene silencing, yeast two-hybrid, *in planta* protein accumulation, and *in vitro* kinase assays were performed as described by Wu *et al.* (2004). Expression of Pto and its mutant derivatives as fusion proteins with GST in *E. coli* was also as described (Wu *et al.*, 2004).

Acknowledgements

This work was initiated at the Center of Engineering Plants for Resistance to Pathogens (Davis, CA, USA) under the supervision of R.W. Michelmore, and supported by National Science Foundation Cooperative Agreement BIR-8920216. We thank Z. Nimchuk and J. Dangl (University of North Carolina) for the *in vivo* myristoylation assay protocol, and A. Heese-Peck and T. Romeis (Freie Universität Berlin, Germany) for discussions. We thank A. Sesma for the pCAMBgfp vector (The Sainsbury Laboratory, Norwich, UK), and O. Koroleva and G. Calder (John Innes Centre, Norwich, UK) for help with confocal microscopy and the protocol for transformation of cell cultures. Part of this work was funded by a Biotechnology and Biological Science Research Council Grant 83/P15081 to J.P.R. The support of the Gatsby Charitable foundation is gratefully acknowledged.

References

Aoyama, T. and Chua, N. (1997) A glucocorticoid-mediated transcriptional induction system in transgenic plants. *Plant J.* **11**, 605–612.

Axtell, M.J. and Staskawicz, B.J. (2003) Initiation of RPS2-specified disease resistance in *Arabidopsis* is coupled to the AvrRpt2-directed elimination of RIN4. *Cell*, **112**, 369–377.

Baker, B., Zambryski, P., Staskawicz, B. and DineshKumar, S.P. (1997) Signaling in plant–microbe interactions. *Science*, **276**, 726–733.

Belkhadir, Y., Nimchuk, Z., Hubert, D.A., Mackey, D. and Dangl, J.L. (2004a) *Arabidopsis* RIN4 negatively regulates disease resistance mediated by RPS2 and RPM1 downstream or independent of the NDR1 signal modulator and is not required for the virulence functions of bacterial type III effectors AvrRpt2 or AvrRpm1. *Plant Cell*, **16**, 2822–2835.

Belkhadir, Y., Subramaniam, R. and Dangl, J.L. (2004b) Plant disease resistance protein signaling: NBS–LRR proteins and their partners. *Curr. Opin. Plant Biol.* **7**, 391–399.

Boisson, B., Giglione, C. and Meinnel, T. (2003) Unexpected protein families including cell defense components feature in the *N*-myristoylome of a higher eukaryote. *J. Biol. Chem.* **278**, 43418–43429.

Boutin, J.A. (1997) Myristoylation. *Cell. Signal.* **9**, 15–35.

Case, R.B., Rice, S., Hart, C.L., Ly, B. and Vale, R.D. (2000) Role of the kinesin neck linker and catalytic core in microtubule-based motility. *Curr. Biol.* **10**, 157–160.

Chang, J.H., Tai, Y.S., Bernal, A.J., Lavelle, D.T., Staskawicz, B.J. and Michelmore, R.W. (2002) Functional analyses of the *Pto* resistance gene family in tomato and the identification of a minor resistance determinant in a susceptible haplotype. *Mol. Plant Microbe. Interact.* **15**, 281–291.

Chiu, W., Niwa, Y., Zeng, W., Hirano, T., Kobayashi, H. and Sheen, J. (1996) Engineered GFP as a vital reporter in plants. *Curr. Biol.* **6**, 325–330.

Chow, M., Newman, J.F.E., Filman, D., Hogle, J.M., Rowlands, D.J. and Brown, F. (1987) Myristylation of picornavirus capsid protein VP4 and its structural significance. *Nature*, **327**, 482–486.

Dangl, J.L. and Jones, J.D.G. (2001) Plant pathogens and integrated defence responses to infection. *Nature*, **411**, 826–833.

Deslandes, L., Olivier, J., Peeters, N., Feng, D.X., Khounlotham, M., Boucher, C., Somssich, I.E., Genin, S. and Marco, Y. (2003) Physical interaction between RRS1-R, a protein conferring resistance to bacterial wilt, and PopP2, a type III effector targeted to the plant nucleus. *Proc. Natl Acad. Sci. USA*, **100**, 8024–8029.

Farazi, T.A., Waksman, G. and Gordon, J.I. (2001) The biology and enzymology of protein *N*-myristoylation. *J. Biol. Chem.* **276**, 39501–39504.

Flor, H.H. (1971) The current status of the gene-for-gene concept. *Annu. Rev. Phytopathol.* **9**, 275–296.

© 2005 The Authors

Hammond-Kosack, K.E. and Jones, J.D.G. (1996) Resistance gene-dependent plant defense responses. *Plant Cell*, **8**, 1773–1791.

Hanks, S.K. and Hunter, T. (1995) The eukaryotic protein kinase superfamily: kinase (catalytic) domain structure and classification. *FASEB J.* **9**, 576–596.

Hantschel, O., Nagar, B., Guettler, S., Kretzschmar, J., Dorey, K., Kuriyan, J. and Superti-Furga, G. (2003) A myristoyl/phosphotyrosine switch regulates c-Abl. *Cell*, **112**, 845–857.

Haseloff, J. and Amos, B. (1995) GFP in plants. *Trends Genet.* **11**, 328–329.

Hayashi, N., Matsubara, M., Jinbo, Y., Titani, K., Izumi, Y. and Matsushima, N. (2002) Nef of HIV-1 interacts directly with calcium-bound calmodulin. *Prot. Sci.* **11**, 529–537.

Horton, R.M., Hunt, H.D., Ho, S.N., Pullen, J.K. and Pease, L.R. (1989) Engineering hybrid genes without the use of restriction enzymes: gene splicing by overlapping extension. *Gene*, **77**, 61–68.

Jia, Y., McAdams, S.A., Bryan, G.T., Hershey, H.P. and Valent, B. (2000) Direct interaction of resistance gene and avirulence gene products confers rice blast resistance. *EMBO J.* **19**, 4004–4014.

Johnson, D.R., Bhatnagar, R.S., Knoll, L.J. and Gordon, J.I. (1994) Genetic and biochemical studies of protein *N*-myristoylation. *Annu. Rev. Biochem.* **63**, 869–914.

Jones, D.A. and Jones, J.D.G. (1996) The role of leucine-rich repeat proteins in plant defences. *Adv. Bot. Res. Adv. Plant Pathol.* **24**, 89–167.

Jones, J.D.G., Shulumukov, L., Carland, F., English, J., Scofield, S.R., Bishop, G.J. and Harrison, K. (1992) Effective vectors for transformation, expression of heterologous genes, and assaying transposon excision in transgenic plants. *Transgen. Res.* **1**, 285–297.

Kim, Y.J., Lin, N.C. and Martin, G.B. (2002) Two distinct *Pseudomonas* effector proteins interact with the Pto kinase and activate plant immunity. *Cell*, **109**, 589–598.

Loh, Y.-T., Zhou, J. and Martin, G.B. (1998) The myristylation motif of Pto is not required for disease resistance. *Mol. Plant Microbe. Interact.* **11**, 572–576.

Lu, R., Malcuit, I., Moffett, P., Ruiz, M.T., Peart, J., Wu, A.-J., Rathjen, J.P., Bendahmane, A., Day, L. and Baulcombe, D.C. (2003) High throughput virus-induced gene silencing implicates heat shock protein 90 in plant disease resistance. *EMBO J.* **22**, 5690–5699.

Mackey, D., Holt, B.F., Wig, A. and Dangl, J.L. (2002) RIN4 interacts with *Pseudomonas syringae* type III effector molecules and is required for RPM1-mediated resistance in *Arabidopsis*. *Cell*, **108**, 743–754.

Mackey, D., Belkhadir, Y., Alonso, J.M., Ecker, J.R. and Dangl, J.L. (2003) *Arabidopsis* RIN4 is a target of the type III virulence effector AvrRpt2 and modulates RPS2-mediated resistance. *Cell*, **112**, 379–389.

Martin, M.L. and Busconi, L. (2000) Membrane localization of a rice calcium-dependent protein kinase (CDPK) is mediated by myristoylation and palmitoylation. *Plant J.* **24**, 429–435.

Martin, G.B., Brommonschenkel, S.H., Chunwongse, J., Frary, A., Ganal, M.W., Spivey, R., Wu, T., Earle, E.D. and Tanksley, S.D. (1993) Map-based cloning of a protein kinase gene conferring disease resistance in tomato. *Science*, **262**, 1432–1436.

Matsubara, M., Titani, K., Taniguchi, H. and Hayashi, N. (2003) Direct involvement of protein myristoylation in myristoylated alanine-rich C kinase substrate (MARCKS)-calmodulin interaction. *J. Biol. Chem.* **278**, 48898–48902.

Maurer-Stroh, S., Eisenhaber, B. and Eisenhaber, F. (2002) *N*-terminal *N*-myristoylation of proteins: refinement of the sequence motif and its taxon-specific differences. *J. Mol. Biol.* **317**, 523–540.

Moscufo, N. and Chow, M. (1992) Myristate–protein interactions in poliovirus: interactions of VP4 threonine 28 contribute to the structural conformation of assembly intermediates and the stability of assembled virions. *J. Virol.* **66**, 6849–6857.

Murase, K., Shiba, S., Iwano, M., Che, F.-S., Watanabe, M., Isogai, A. and Takayama, S. (2004) A membrane-anchored protein kinase involved in *Brassica* self-incompatibility signaling. *Science*, **303**, 1516–1519.

Nimchuk, Z., Marois, E., Kjemtrup, S., Leister, R.T., Katagiri, F. and Dangl, J.L. (2000) Eukaryotic fatty acylation drives plasma membrane targeting and enhances function of several type III effector proteins from *Pseudomonas syringae*. *Cell*, **101**, 353–363.

Pedley, K.F. and Martin, G.B. (2003) Molecular basis of Pto-mediated resistance to bacterila speck disease in tomato. *Annu. Rev. Phytopathol.* **41**, 215–243.

Qi, Q., Rajala, R.V.S., Anderson, W., Jiang, C., Rozwadowski, K., Selvaraj, G., Sharma, R. and Datla, R. (2000) Molecular cloning, genomic organization, and biochemical characterization of myristoyl-CoA:protein *N*-myristoyltransferase from *Arabidopsis thaliana*. *J. Biol. Chem.* **275**, 9673–9683.

Ratcliff, F., Martin-Hernandez, A.M. and Baulcombe, D.C. (2001) Tobacco rattle virus as a vector for analysis of gene function by silencing. *Plant J.* **25**, 237–245.

Rathjen, J.P. and Moffett, P. (2003) Early signal transduction events in specific plant disease resistance. *Curr. Opin. Plant Biol.* **6**, 300–306.

Rathjen, J.P., Chang, J.H., Staskawicz, B.J. and Michelmore, R.W. (1999) Constitutively active Pto induces a *Prf*-dependent hypersensitive response in the absence of avrPto. *EMBO J.* **18**, 3232–3240.

Resh, M.D. (1999) Fatty acylation of proteins: new insights into membrane targeting of myristoylated and palmitoylated proteins. *Biochim. Biophys. Acta*, **1451**, 1–16.

Riely, B.K. and Martin, G.B. (2001) Ancient origin of pathogen recognition specificity conferred by the tomato disease resistance gene Pto. *Proc. Natl Acad. Sci. USA*, **98**, 2059–2064.

Rommens, C.M.T., Salmeron, J.M., Baulcombe, D.C. and Staskawicz, B.J. (1995) Use of a gene expression system based on potato virus X to rapidly identify and characterize a tomato *Pto* homolog that controls fenthion sensitivity. *Plant Cell*, **7**, 249–257.

Ronald, P.C., Salmeron, J.M., Carland, F.M. and Staskawicz, B.J. (1992) The cloned avirulence gene *AvrPto* induces disease resistance in tomato cultivars containing the *Pto* resistance gene. *J. Bacteriol.* **174**, 1604–1611.

Salmeron, J.M., Barker, S.J., Carland, F.M., Mehta, A.Y. and Staskawicz, B.J. (1994) Tomato mutants altered in bacterial disease resistance provide evidence for a new locus controlling pathogen recognition. *Plant Cell*, **6**, 511–520.

Salmeron, J.M., Oldroyd, G.E.D., Rommens, G.M.T., Scofield, S.R., Kim, H.S., Lavelle, D.T., Dahlbeck, D. and Staskawicz, B.J. (1996) Tomato *Prf* is a member of the leucine-rich repeat class of plant disease resistance genes and lies embedded within the *Pto* kinase gene cluster. *Cell*, **86**, 123–133.

Sambrook, J., Fritsh, E.F. and Maniatis, T. (1989) *Molecular Cloning: A Laboratory Manual*, 3rd edn. Cold Spring Harbor, NY, USA: Cold Spring Harbor Laboratory Press.

Schagger, H. and Von Jagow, G. (1987) Tricine-sodium dodecyl sulfate-polyacrylamide gel electrophoresis for the separation of proteins in the range from 1 to 100 kDa. *Anal. Biochem.* **166**, 368–379.

Scofield, S.R., Tobias, C.M., Rathjen, J.P., Chang, J.H., Lavelle, D.T., Michelmore, R.W. and Staskawicz, B.J. (1996) Molecular basis of gene-for-gene specificity in bacterial speck of tomato. *Science*, **274**, 2063–2065.

© 2005 The Authors
Journal compilation © 2005 Blackwell Publishing Ltd,

Sesma, A. and Osbourn, A.E. (2004) The rice leaf blast pathogen undergoes developmental processes typical of root-infecting fungi. *Nature*, **431**, 582–586.

Sessa, G., D'Ascenzo, M. and Martin, G.B. (2000) Thr-38 and Ser-198 are Pto autophosphorylation sites required for the AvrPto-Pto-mediated hypersensitive response. *EMBO J.* **19**, 2257–2269.

Shan, L., Thara, V.K., Martin, G.B., Zhou, J.-M. and Tang, X. (2000) The *Pseudomonas* AvrPto protein is differentially recognised by tomato and tobacco and is localised to the plant plasma membrane. *Plant Cell*, **12**, 2323–2337.

Shao, F., Golstein, C., Ade, J., Stoutemyer, M., Dixon, J.E. and Innes, R.W. (2003) Cleavage of Arabidopsis PBS1 by a bacterial type III effector. *Science*, **301**, 1230–1233.

Swiderski, M. and Innes, R.W. (2001) The *Arabidopsis PBS1* resistance gene encodes a member of a novel protein kinase subfamily. *Plant J.* **26**, 101–112.

Tang, X., Frederick, R.D., Zhou, J., Halterman, D.A., Jia, Y. and Martin, G.B. (1996) Initiation of plant disease resistance by physical interaction of AvrPto and Pto kinase. *Science*, **274**, 2060–2063.

Ulrich, A., Schmitz, A.A.P., Braun, T., Yuan, T., Vogel, H.J. and Vergeres, G. (2000) Mapping the interface between calmodulin and MARCKS-related protein by fluorescence spectroscopy. *Proc. Natl Acad. Sci. USA*, **97**, 5191–5196.

Vleeshouwers, V.G.A.A., Martens, A., Van Dooijeweert, W., Colon, L.T., Govers, F. and Kamoun, S. (2001) Ancient diversification of the Pto kinase family preceded speciation in *Solanum*. *Mol. Plant Microbe. Interact.* **14**, 996–1005.

Wu, A.-J., Andriotis, V.M.E., Durrant, M.C. and Rathjen, J.P. (2004) A patch of surface-exposed residues mediates negative regulation of immune signaling by tomato Pto kinase. *Plant Cell*, **16**, 2809–2821.

Wulf, J., Pascuzzi, P.E., Fahmy, A., Martin, G.B. and Nicholson, L.K. (2004) The solution structure of type III effector protein AvrPto reveals conformational and dynamic features important for plant pathogenesis. *Structure*, **12**, 1257–1268.

Zhou, J., Loh, Y.Y., Bressan, R.A. and Martin, G.B. (1995) The tomato gene *Pti1* encodes a serine/threonine kinase that is phosphorylated by Pto and is involved in the hypersensitive response. *Cell*, **83**, 925–935.

© 2005 The Authors
Journal compilation © 2005 Blackwell Publishing Ltd,